Journal of Structural Geology, Vol. 12, No. 1, pp. 99 to 111, 1990
Printed in Great Britain

0191-8141/90 $03.00 + 0.00

Proterozoic contact relationships between gneissic basement and metasedimentary cover in the Needle Mountains, Colorado, U.S.A.

RICHARD G. GIBSON

Amoco Research Center, P. O. Box 3385, Tulsa, OK 74102, U.S.A.

(*Received* 1 *December* 1987; *accepted in revised form* 15 *April* 1989)

Abstract—In the Needle Mountains of southwestern Colorado, Proterozoic siliciclastic metasedimentary rocks of the Uncompahgre Group occupy a synclinorium bounded by 1690+ Ma gneissic and plutonic basement rocks. Stratigraphic facing of the Uncompahgre Group away from basement and local preservation of erosional features along the basement–cover interface imply that the contact is an unconformity. A ≤12 m thick zone of phyllite, which commonly contains textural evidence of derivation from basement lithologies, occurs everywhere along the contact. Tectonic fabrics within and near the contact zones locally record non-coaxial deformation that resulted from upward movement of the cover relative to basement on each side of the synclinorium. Comparison of bulk chemistries of basement and contact zone samples indicates that hydration and the loss of CaO, MgO, SiO_2 and Na_2O accompanied alteration of plagioclase + quartz + biotite-bearing basement rocks to muscovite + quartz + Fe/Ti-oxide ± choritoid ± andalusite ± chlorite phyllites. The micaceous zone along the contact is interpreted as a metamorphosed regolith that localized out-of-synform movement during folding of the basement and its parautochthonous cover. Localization of intense deformation within mechanically weak lithologic horizons, such as regoliths, along basement–cover contacts can occur in situations where there is little relative displacement of the adjacent rocks and the stratigraphic significance of the boundary is preserved. Detailed petrographic and kinematic analysis may help distinguish such contacts from major fault boundaries.

INTRODUCTION

RECONSTRUCTING the geologic history of deformed and metamorphosed geologic terranes requires an understanding of the nature and significance of contacts between supracrustal sequences and adjacent metamorphic complexes. The recognition of erosional features, basal conglomerates, and/or clasts of the metamorphic complex within the supracrustal sequence supports the interpretation of such contacts as unconformities. However, where locally intense or complex deformation is present along such boundaries (e.g. Coney 1980, Gee 1980, Gratier & Vialon 1980, Jacob *et al.* 1983, Lambert & van Staal 1987), it is important to distinguish between deformation zones that signify zones of major displacement or disrupt original stratigraphic relationships, and those of minor displacement across which primary stratigraphic relationships are preserved.

Early to Middle Proterozoic rocks in the northwestern Needle Mountains of southwestern Colorado (Fig. 1) comprise two contrasting lithologic assemblages, a volcano-plutonic complex and a siliciclastic sedimentary sequence. The presence of localized penetrative deformation along the contacts between these assemblages has hindered interpretation of their original stratigraphic relationships and, thus, relative ages. Previous workers have interpreted the contacts as either faulted unconformities (Cross *et al.* 1905, Barker 1969) or Proterozoic thrust faults (Tewksbury 1985). Recent studies in this area (Gibson 1987, Harris 1987, in press, Harris *et al.* 1987, Gibson & Simpson 1988) have concluded that the structural and kinematic histories of both lithologic assemblages can be best explained if the volcano-plutonic complex comprised depositional basement to the sedimentary cover. Field, microstructural and geochemical data from the basement–cover contacts, presented in this paper, substantiate this interpretation and indicate that the contacts are segments of an unconformity with an underlying regolith that localized ductile deformation.

GEOLOGIC SETTING

The study area is located in the northwestern part of the Needle Mountains (Fig. 1a), a 1100 km^2 exposure of Proterozoic rocks surrounded by Paleozoic sedimentary rocks and Tertiary volcanogenic rocks in southwestern Colorado. Proterozoic basement in the study area (Fig. 1b) consists of a layered gneiss complex (Animas River Gneiss Suite of Gibson & Harris in press) intruded by granite plutons. The gneiss complex is composed predominantly of plagioclase + quartz + biotite ± potassium feldspar ± epidote ± muscovite ± hornblende ± garnet gneiss and hornblende + plagioclase ± epidote ± biotite ± quartz gneiss with rare primary features indicative of felsic and mafic volcanogenic and plutonic protoliths (Barker 1969, Gibson & Simpson 1988). U–Pb zircon and Rb–Sr whole-rock geochronology yield ages of approximately 1755 Ma for part of the gneiss complex and about 1690 Ma for the granite plutons (ages recalculated from Silver & Barker 1968, Barker *et al.* 1969, Bickford *et al.* 1969). Proterozoic cover rocks of the Uncompahgre Group (Gibson & Harris in press) com-

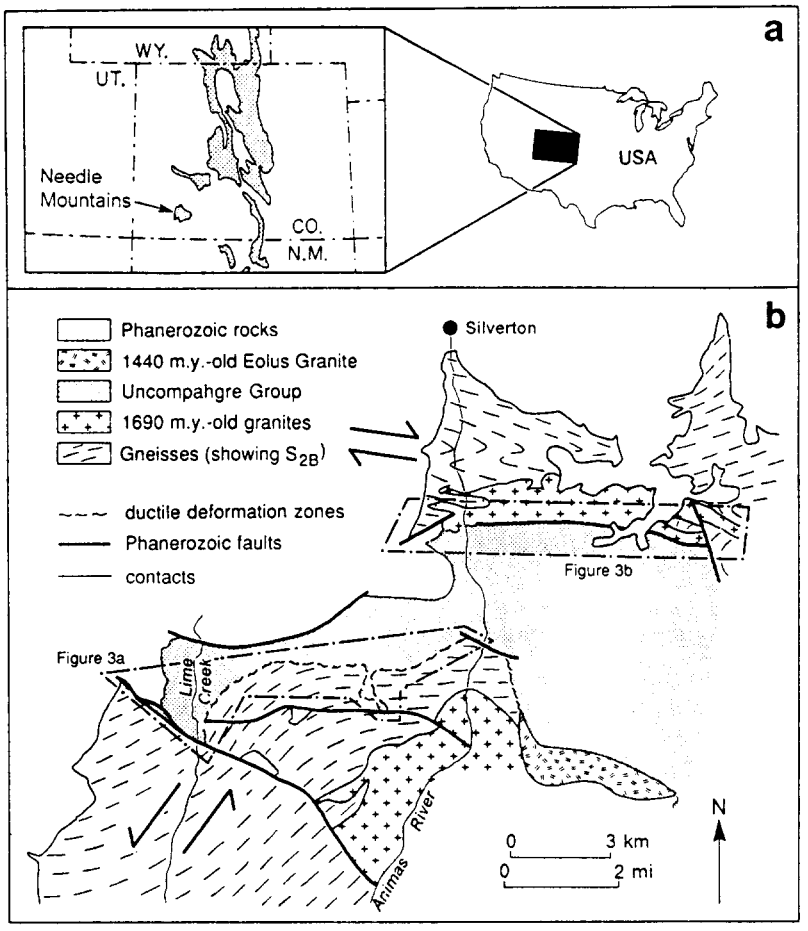

Fig. 1. (a) Location of Needle Mountains; stippled areas are regions of Middle Proterozoic to Archean outcrop. (b) Geologic map of northwestern Needle Mountains simplified from Harris *et al.* (1977); split arrows indicate zones of dextral and sinistral shear defined by Gibson & Simpson (1988).

prise a sequence at least 3 km thick and occupy an E–W-trending outcrop belt bounded on both the north and south by basement (Fig. 1b). The internal stratigraphy of the Uncompahgre Group consists of four quartzite (Q_1–Q_4) and five pelite (P_1–P_5) units with well-preserved primary sedimentary structures (Harris 1987, Harris & Eriksson 1987). Most of the sequence was deposited in a shallow marine setting, although the lowest part of the basal quartzite unit (Q_1) is probably alluvial in origin (Harris & Eriksson 1987).

Harris *et al.* (1987), Gibson & Simpson (1988) and Harris (in press) have documented the polyphase structural evolution of this area. Rocks of the gneiss complex were polydeformed (D_B) and metamorphosed (M_B) prior to intrusion of the ~1690 Ma granites. D_B deformation culminated with formation of a penetrative S_{2B} foliation and mineral lineation, defined by quartz and feldspar ribbons and aligned biotite or amphibole, in rocks of the gneiss complex. Subsequent D_{BC} deformation affected the gneiss complex, granites and Uncompahgre Group. An initial phase of N-directed thrusting was localized in rocks of the Uncompahgre Group stratigraphically above the middle Q_1 (Harris in press). Thrusting was progressively followed by folding of both the cover rocks and basement gneisses about subhorizontal E–W-trending axes, and development of an E-striking subvertical foliation in the granites (Harris *et al.* 1987). Mapping within the Uncompahgre Group has shown that its outcrop belt is a synclinorium (Cross *et al.* 1905, Barker 1969, Tewksbury 1985) that has been interpreted as a cuspate structure formed during contemporaneous D_{BC} folding of the basement and cover (Harris *et al.* 1987). NNW-shortening during D_{BC} was partly accommodated by movement along ESE-striking dextral and NE-striking sinistral conjugate strike-slip shear zones (Gibson & Simpson 1988). Zones of major dextral and sinistral shearing within the basement, as delineated by the regionally sigmoidal geometry of S_{2B}, mesoscopic shear indicators and quartz petrofabrics, are shown in Fig. 1(b). A second metamorphic episode, M_{BC}, caused syn- to post-D_{BC} porphyroblast growth and annealing of minerals in both the basement and cover rocks. The minimum ages of D_{BC} and M_{BC} are constrained by emplacement of the undeformed ~1440 Ma Eolus Granite, exposed south and east of the study area (Fig. 1b).

BASEMENT–COVER CONTACTS

Previous workers in the Needle Mountains have documented that the Uncompahgre Group is typically in contact with the basement gneisses and granites along a zone of foliated micaceous rock (phyllonite of Barker

1969, Tewksbury 1985). Cross *et al.* (1905) mapped these contacts as faults but interpreted the Uncompahgre Group to be younger than the gneiss complex. Barker (1969) concluded that the contacts are part of an unconformity at the base of the Uncompahgre Group, but recognized that portions of the southern contact may be a thrust fault. Tewksbury (1985) examined the microstructures in rocks along the contacts and concluded that they resemble those found in ductile shear zones; she interpreted the contacts as fault zones and argued that the relative ages of rocks on either side could not be constrained. On the basis of the fault zone interpretation, Tewksbury (1985) proposed a fold-thrust belt model for the evolution of this area, in which both the northern and southern basement–cover contacts are S-verging thrust faults (Fig. 2a). Harris *et al.* (1987) have questioned this interpretation and suggested that the contacts are unconformities that localized deformation during infolding of cover rocks into basement during D_{BC} (Fig. 2b).

Portions of the basement–cover contacts lack the micaceous zone and are characterized by fractures, iron staining and local cataclastic textures that overprint older penetrative tectonic fabrics in the adjacent rocks. These contacts are interpreted as fault zones. On the basis of facies and thickness variations in the Paleozoic sedimentary rocks, Baars & See (1968) and Spoelhof (1976) demonstrated that some of these faults underwent episodic movement throughout much of the Paleozoic and, possibly, into the Tertiary. Precise ages of movement on fault segments that do not affect the Paleozoic or Tertiary sequences are unknown. Because the aim of this study was to evaluate the pre-deformational relationships along the Proterozoic basement–cover contacts and the nature of Proterozoic deformation along these boundaries, portions of the contacts that have been modified by Phanerozoic faulting are not discussed further.

Contact geometry

Maps and cross-sections of the northern and southern basement–cover contacts, showing fabric orientations and outcrop locations, comprise Fig. 3. The southern contact, east of cross-section B–B′ (Fig. 3b), is subhorizontal at high elevations (south of Snowdon Peak) and steepens in dip toward the north. It is markedly convex-upward in shape. West of section B–B′ (Fig. 3b), the contact curves to a N–S strike (along Lime Creek) and varies from steeply SE-dipping to W-dipping. East of the Animas River, the deformed zone defining the southern contact is cross-cut by the ~1440 Ma Eolus Granite (Barker 1969, Tewksbury 1985), indicating that it is a Middle Proterozoic feature.

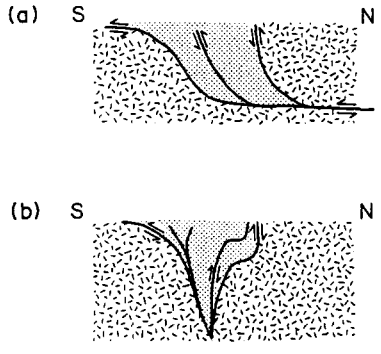

Fig. 2. Possible interpretations of basement–cover relationships in the northwestern Needle Mountains displayed in schematic N–S cross-sections along the Animas River: (a) fold-thrust belt model after Tewksbury (1985); (b) cuspate fold model after Harris *et al.* (1987).

The northern contact zone is vertical in the bottom of the Animas River canyon (Fig. 3a) and dips steeply northward at higher elevations on the western canyon walls. Thus, it also has a slightly convex-upward form. At location I (Fig. 3a), the contact zone is unconformably overlain by conglomerates of the Upper Cambrian Ignacio Formation. Its similarity to the southern contact, however, suggests that the northern contact is also of Middle Proterozoic (>1440 Ma) age.

Away from the Phanerozoic faults, the basement and cover are everywhere separated from one another by a zone of quartz + muscovite + Fe/Ti-oxide ± chloritoid ± andalusite ± chlorite rock that attains a maximum thickness of approximately 12 m south of Snowdon Peak (Fig. 3b) but is more typically less than 6 m thick. This zone is parallel to bedding in the adjacent Uncompahgre Group and is generally oblique to S_{2B} in the basement gneisses (Fig. 3). The basal stratigraphic unit (Q_1) of the Uncompahgre Group is everywhere in contact with basement except along the N- to NE-striking segment of the contact immediately east of Lime Creek (Fig. 3b), where younger quartzites and pelites of the Uncompahgre Group are juxtaposed with basement (Harris *et al.* 1987). Cross-bedding in the Uncompahgre Group invariably indicates facing away from the basement (Harris *et al.* 1987).

Mesoscopic and microscopic characteristics

Micaceous rocks exposed along the basement–cover contacts typically contain a prominent muscovite foliation, S_M, and are best described as phyllites. The term 'phyllite' is used here, instead of 'phyllonite' (Barker 1969, Tewksbury 1985), as a non-genetic term to denote these fine-grained, muscovite-rich rocks because: (1) their protoliths are not always determinable: and (2) their fine grain size may not be due entirely to mechanical grain size reduction of their protoliths (cf. American Geological Institute 1980). Along the northern contact, S_M dips moderately to steeply northward (Fig. 4a). Along N-dipping segments of the southern contact, S_M dips as much as 20° more steeply northward than the contact surface; poles to S_M define a girdle distribution (Fig. 4b) because of the variable orientation of the contact zone. S_M surfaces typically contain a faint down-dip muscovite lineation, L_M (Fig. 4). Gently to moderately plunging crenulation folds locally deform S_M along both contacts, but are of very limited distribution within the phyllite and are not present in the adjacent basement or cover rocks.

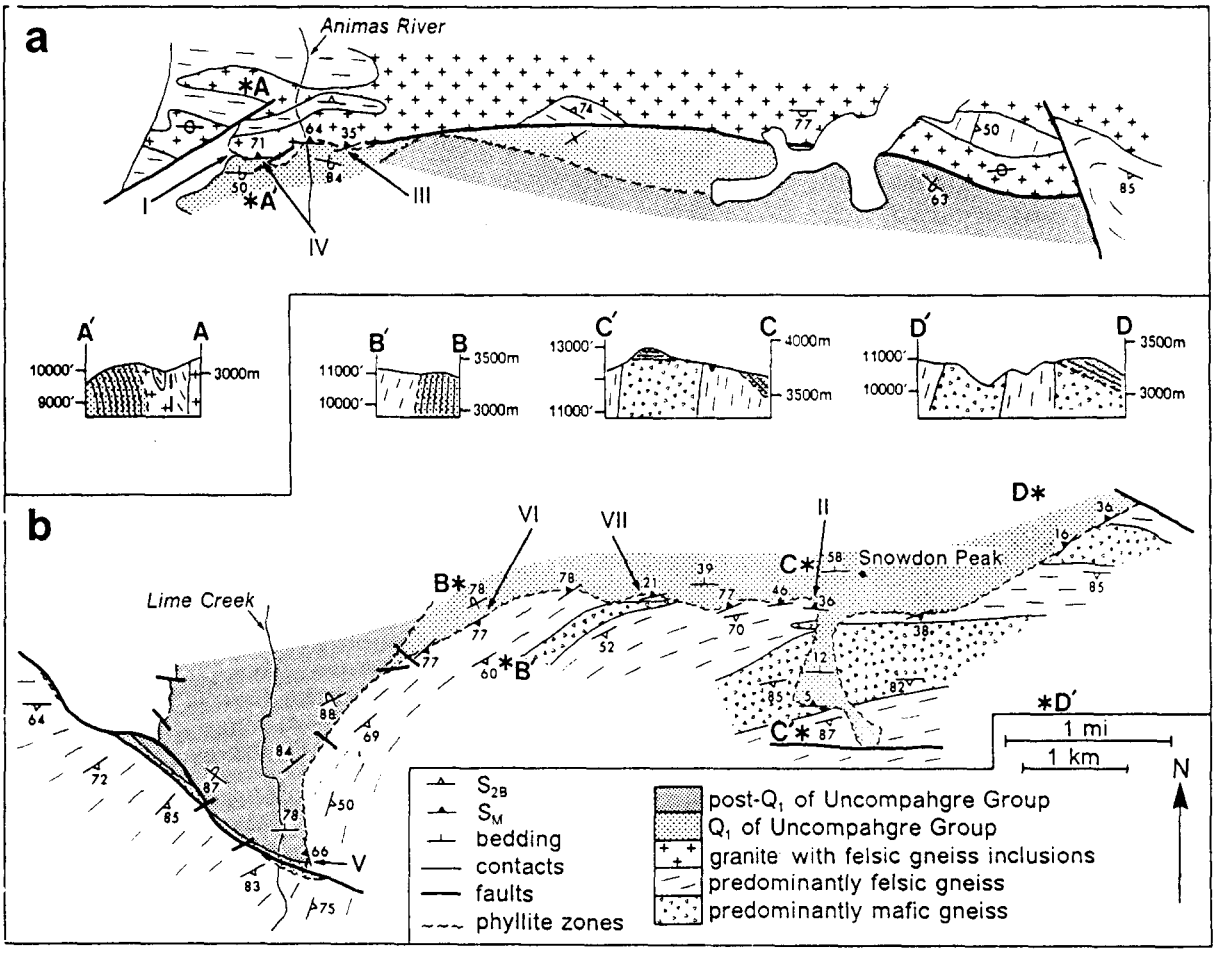

Fig. 3. Strip maps and cross-sections of (a) northern and (b) southern basement–cover contacts. Map locations correspond to boxed areas in Fig. 1(b) and Roman numerals denote outcrop locations cited in text.

On the basement side of the contact zones, S_M overprints S_{2B} in the gneisses (Fig. 5a) and is defined by spaced (Powell 1979) domains of ≤0.1 mm long, aligned muscovite grains. In the lithons between these folia, S_{2B} is preserved as alternating quartz ribbons and bands of non-systematically aligned muscovite (Fig. 5b). The relict S_{2B} fabric is variably oriented with respect to S_M and is mildly crenulated when the two fabrics are at high angles to one another. Aggregates of euhedral ilmenite ± quartz ± chlorite comprise tabular arrays that mimic the morphology of biotite grains in the protolith felsic gneisses (Fig. 5c). Within ~1 m of the Uncompahgre Group, S_{2B} is generally not visible and S_M is more penetrative, defined by a continuous muscovite alignment that anastomoses around quartz grains (Fig. 5e). Granites adjacent to the northern contact are locally transformed into muscovite-rich phyllites containing fractured and altered feldspar porphyroclasts (Fig. 5d).

At several well-exposed localities (e.g. II and IV, Fig. 3), the boundary between the Uncompahgre Group conglomerates and adjacent micaceous zone is abrupt and undulatory (Fig. 7). Because of variable exposure, it is unknown if such irregularities are everywhere typical of the contacts. At location II, S_M in the micaceous zone locally continues into the base of the overlying massive conglomerate (Fig. 7a). In contrast, deformation features are absent immediately along the contact surface at location IV (Fig. 3a), where the massive basal conglomerate of the Uncompahgre Group is adjacent to a non-foliated, tan, micaceous lithology (Fig. 7b). This micaceous zone contains lenticular domains up to 75 cm long of relict S_{2B} and coarse-grained granitic texture (Fig. 7b). In thin section, plutonic textures are preserved within the granite lenses, despite replacement of primary feldspar by fine-grained muscovite aggregates (Fig. 5f). Portions of the micaceous zone lacking these

Fig. 5. (a) S_M superimposed on S_{2B} in outcrop of retrograded felsic gneiss along southern contact. (b) Spaced S_M domains cross-cutting S_{2B}; muscovite-rich areas between quartz ribons show no preferential mineral alignment (similar to Fig. 5f); plane light. (c) Anastomosing S_M domains oblique to relict S_{2B} in retrograded felsic gneiss; note ilmenite + chlorite pseudomorph after biotite (arrow); plane light. (d) Fractured and altered feldspar porphyroclast in phyllite derived from granite; arrows indicate inferred sense of shear; crossed nicols. (e) Continuous S_M fabric defined by muscovite wrapping around quartz grains; plane light. (f) Relict crystal outlines of primary feldspar grains preserved by muscovite grain size variation in retrograded granite; dark chloritoid grains (Ctd) occur intergrown with muscovite; crossed nicols.

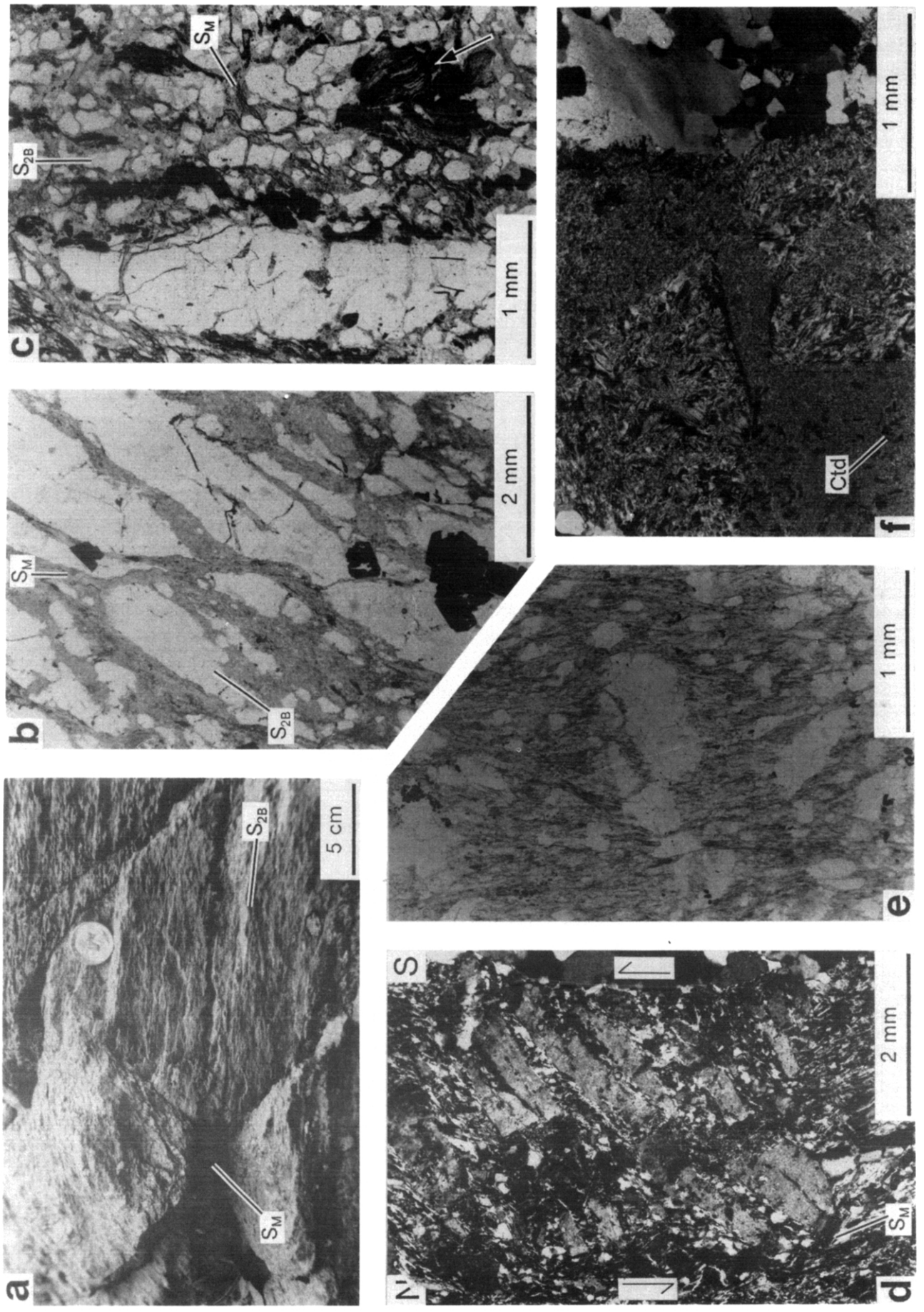

Fig. 5.

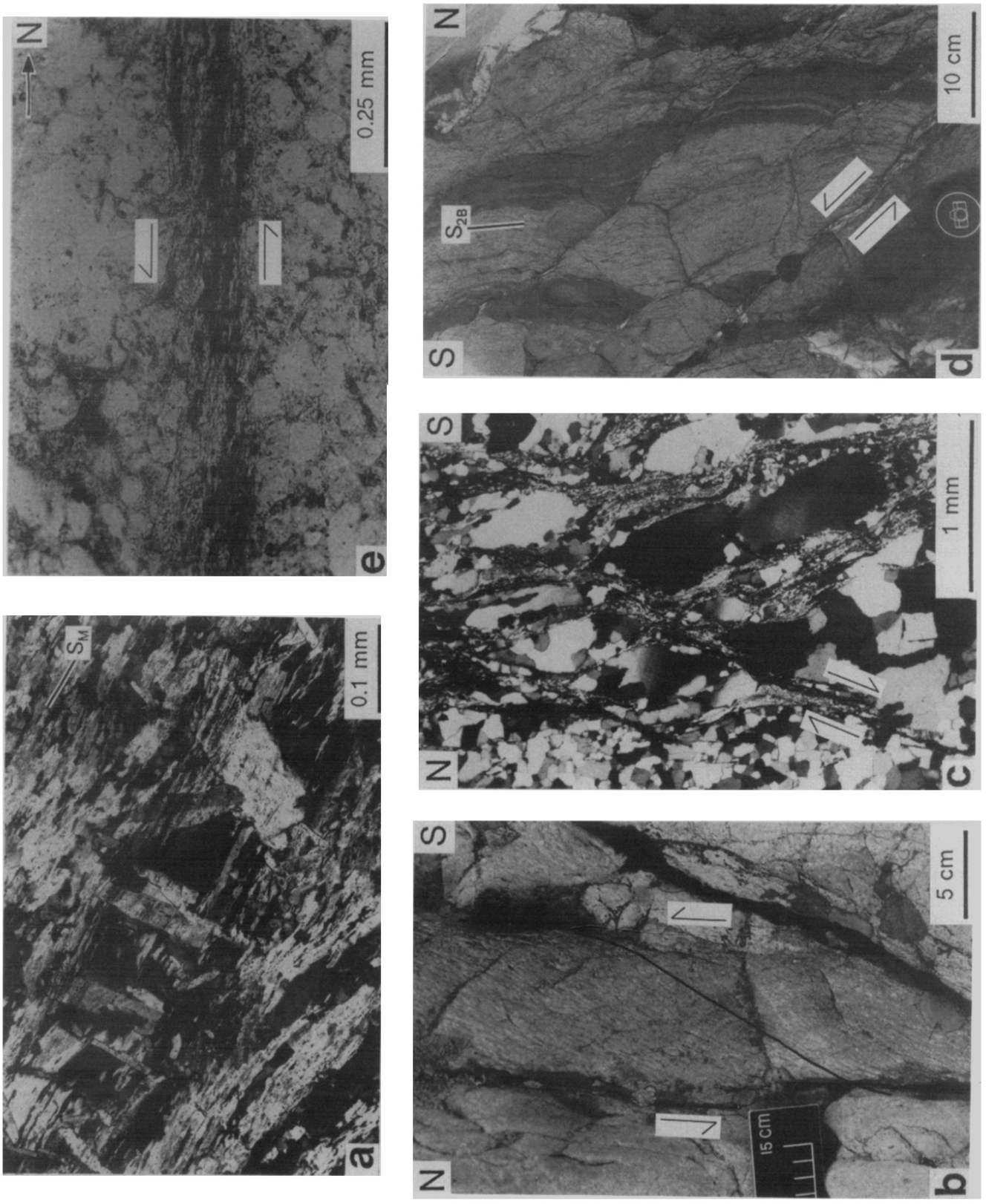

Fig. 6.

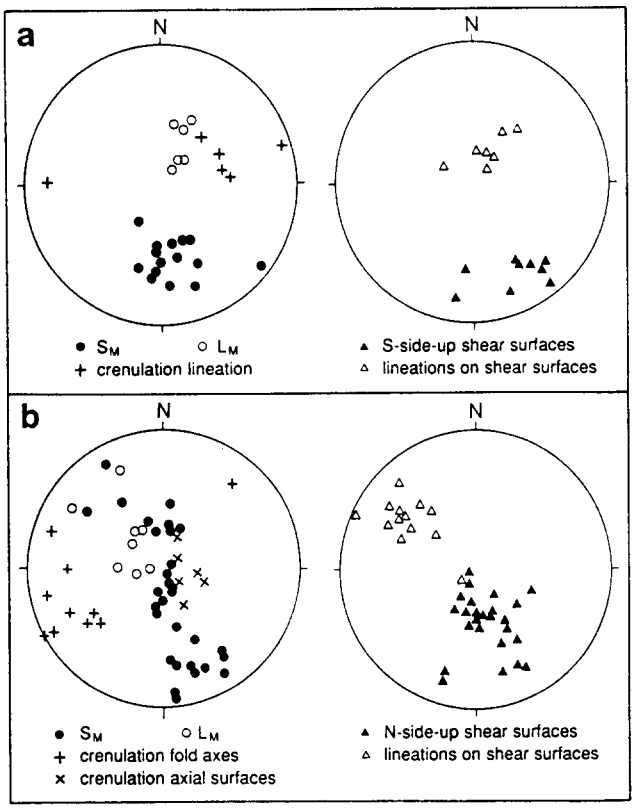

Fig. 4. Orientation data for fabric elements in rocks along northern (a) and southern (b) basement–cover contacts; lower-hemisphere equal-angle projections.

relict textures consist of equant quartz aggregates surrounded by a matrix of randomly oriented, fine-grained muscovite. Approximately 0.5 m north of the contact, S_M appears as a gently N-dipping foliation that intensifies and steepens in dip toward a covered interval that separates this outcrop from non-retrograded basement rocks exposed several meters farther north (Fig. 7b). Compositional layering, defined by varying proportions of muscovite, chlorite and chloritoid, and comparable in scale to layering in the adjacent gneiss complex, also occurs in other weakly foliated micaceous lithologies along the northern contact near location IV.

Equant and ribbon-shaped quartz aggregates within the phyllites are generally polycrystalline and polygonal with little optically visible, non-recovered crystal-plastic strain, even in the hinges of crenulation folds. Blocky quartz grains locally enclose trails of muscovite or ilmenite that are aligned parallel to S_M. Undeformed, randomly oriented porphyroblasts of muscovite (Fig. 6a), chloritoid, andalusite, chlorite and magnetite overgrow all of the deformation fabrics in many phyllite samples. Such mineral assemblages occur in samples either lacking or containing the relict S_{2B} basement fabric. In some specimens from the northern contact, hematite pseudomorphs after magnetite are bounded by short, straight, fibrous quartz pressure shadows elongate parallel to S_M.

Basal Uncompahgre Group quartzites and conglomerates contain a penetrative foliation only locally within ~1 m of the contact with basement. This fabric is defined by a bedding-parallel clast alignment, anastomosing fine-grained muscovite folia, and mica beards adjacent to detrital quartz grains.

The N- to NE-striking segment of the southern contact east of Lime Creek (Fig. 3b) is unique because Uncompahgre Group rocks younger than Q_1 are adjacent to basement (Harris *et al.* 1987). Poor exposure allowed examination of only one outcrop along this segment. At location V (Fig. 3b), S_M in retrograded gneisses varies from vertical to W-dipping and contains a

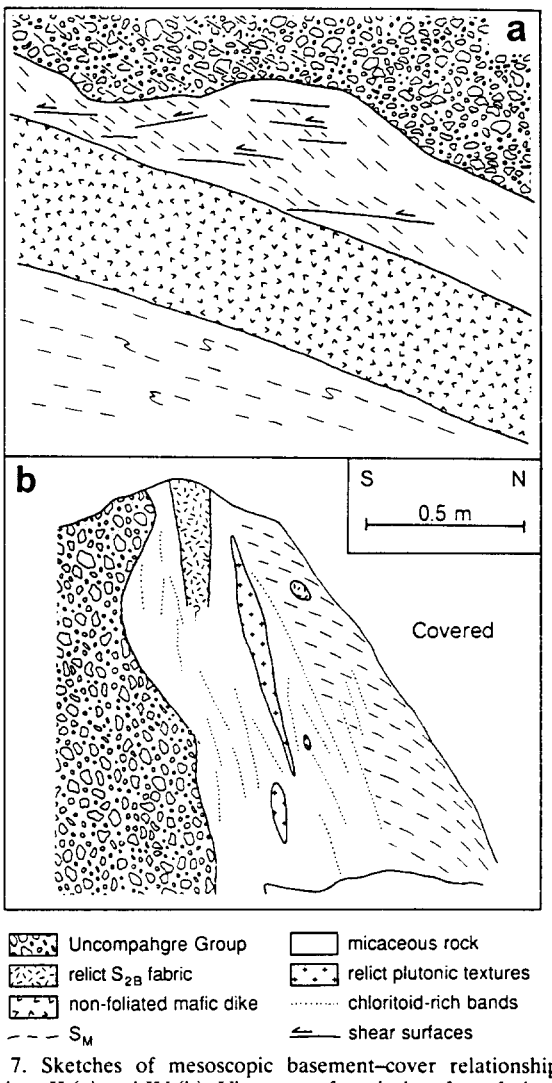

Fig. 7. Sketches of mesoscopic basement–cover relationships at locations II (a) and IV (b). Views are of vertical surfaces facing west and are the same scale. Note foliation in conglomerate in upper left portion of (a). See text for discussion.

Fig. 6. (a) S_M, defined by trails of fine-grained ilmenite, overgrown by muscovite porphyroblasts; crossed nicols. (b) South-side-up bedding-parallel shear zone in Uncompahgre Group near northern contact along Animas River; black line highlights foliation orientation within zone. (c) North-side-up shear bands and σ-type quartz porphyroclasts in deformed Uncompahgre Group conglomerate along southern contact at location II (Fig. 3b); crossed nicols. (d) North-side-up quartz + chlorite shear zones cross-cutting compositional layering in retrograded gneiss along southern contact at location VI (Fig. 3b); (e) Sinistral shear zone in retrograded gneiss at location IV (Fig. 3b); plane light.

mineral lineation plunging approximately 40° toward 195°.

Kinematic indicators

Asymmetric sense-of-shear indicators (Simpson & Schmid 1983) are rare in phyllites from the northern contact zone. West of the Animas River (Fig. 3a), the superposition of S_M onto S_{2B} produced a fabric that can be mistaken for shear bands in outcrop but does not have the sigmoidal geometry of shear bands when examined in thin section (Fig. 5b). Mica beards adjacent to quartz grains generally have orthorhombic symmetry in sections cut normal to S_M and parallel to L_M (Fig. 5e). The down-dip mineral lineation (Fig. 4a) and sense of foliation deflection into the phyllite zone at locations III and IV (Fig. 7b), however, suggest a south-side-up component of shearing during phyllite formation. This sense of shear is verified by fractured feldspar porphyroclasts in deformed granites (Fig. 5d) and rare shear bands that deform S_M. Crystallographic preferred orientation patterns (*c*-axes) from quartz aggregates in these phyllites do not appear to be clearly related to S_M and L_M (Gibson 1987) and, thus, yield no kinematic information.

Within 20 m of the northern contact, steeply S-dipping shear zones up to 10 cm thick and slickensided surfaces with down-dip mineral lineations occur within the Uncompahgre Group (Fig. 4a). The shear zones contain an internally sigmoidal foliation defined by quartz ribbons and muscovite that merges asymptotically into bedding (Fig. 6b). The foliation dips more gently northward than the shear zone margins (bedding), indicating south-side-up movement. Steps on discrete slip surfaces that locally transect bedding at a low angle also indicate south-side-up displacement. Undeformed andalusite grains and polygonal quartz fabrics characterize both the shear zones and slickensided surfaces.

Rocks along the southern contact only display abundant asymmetric kinematic indicators at high elevations south of Snowdon Peak, where the contact is subhorizontal to gently N-dipping (Fig. 3b). Shear bands and retort-shaped quartz aggregates (Fig. 6c) with the geometry of σ-type porphyroclasts (Passchier & Simpson 1986) consistently indicate north-side-up movement within the phyllite zones. This sense of movement is substantiated by the sense of asymmetry of the central segment of a crossed girdle quartz *c*-axis fabric pattern (Fig. 8) for a sample from location II (cf. Schmid & Casey 1986). At location VI, gently N-dipping, S-directed, $\leq$1 cm wide shear zones are the most prominent features (Fig. 6d), but conjugate shear bands are also visible in thin section. Farther west along the steeply-dipping, NE-striking section of the contact (Fig. 3b), asymmetric kinematic indicators are largely absent. Along the N-striking segment of the contact at location V (Fig. 3b), $\leq$1 mm thick, muscovite- and chlorite-rich, sinistral shear zones occur within the mildly retrograded gneisses (Fig. 6e).

Numerous shear zones, similar to those near the northern contact but typically lacking andalusite, occur in the Uncompahgre Group within 10 m of the southern contact. The majority of these zones dip northward, subparallel to bedding, and contain a moderately NW-plunging mineral lineation (Fig. 4b) defined by quartz ribbons and muscovite. Foliation asymmetry and slickenside steps indicate oblique north-side-up and dextral motion. Subvertical, E-striking, south-side-up shear zones are also present, but are much less common.

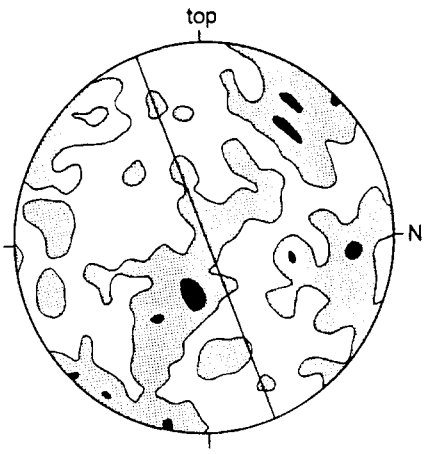

Fig. 8. Quartz *c*-axis preferred orientation for sample from loction II contoured at one (stippled) and three (black) points per 0.36% area (274 measurements) on lower-hemisphere equal-area projection. S_M is shown as solid line with L_M at edge of projection.

DISCUSSION

Deformation along basement–cover contacts

Kinematic indicators in the contact zones and immediately adjacent rocks record upward movement of the Uncompahgre Group relative to basement in opposite directions on the northern and southern contacts. This implies the formation of S_M in zones of non-coaxial deformation, for which microstructural evidence is best preserved along gently to moderately dipping portions of the southern contact. The absence of lithologic markers oblique to the basement–cover contacts precludes determination of the displacement magnitude across them at any given location. Because folding of S_M is restricted to within the phyllite zones, it is interpreted to have occurred progressively within a shear regime (e.g. Platt 1983). Steeply dipping portions of both the northern and southern contacts, however, display an abundance of symmetrical kinematic indicators, including symmetrical mica beards, conjugate shear bands, and straight fibrous pressure fringes. This suggests that these segments experienced either a coaxial strain history or a late-stage coaxial overprint.

The opposed movement senses on the northern and southern contacts imply that the basal part of the Uncompahgre Group is parautochthonous upon basement and has not been tectonically transported a significant distance from its site of deposition, as implied in the model shown in Fig. 2(a). Rather, the opposed move-

ment senses are more consistent with out-of-synform movement during D_{BC} folding of the basement and cover (Fig. 2b). In this model, portions of the initially subhorizontal basement–cover contact were reoriented toward a vertical attitude on the limbs of the cuspate synclinorium. Reorientation caused interlayer slip along mechanically weak lithologic horizons (the contact zones) during folding, a process analogous to flexural slip during concentric folding (Ramsay 1967, Dahlstrom 1977). The final strain increments, however, involved shortening approximately normal to these horizons on the fold limbs, in the same manner that parallel folds become flattened during progressive deformation (Ramsay 1962). This model can account for both the determined movement senses along the contact zones and the apparaent coaxial overprint along steeply dipping contact segments.

Observations from location IV (Fig. 7b) are also consistent with this model. The relationships preserved at this outcrop, including the contact irregularity, lack of deformation along the contact surface and preservation of basement fabrics within the retrograded zone only centimeters from the conglomerate, are most simply interpreted as features of an unconformity at the base of the Uncompahgre Group. This intact portion of the depositional contact was probably preserved either: (1) as a lens within the deformation zone; or (2) along the margin of the phyllite zone where it deviated from its typical position along the contact surface.

Because early-D_{BC}, N-directed thrusting caused some translation and imbrication within the Uncompahgre Group (Harris *et al.* 1987, Harris in press), it is conceivable that N-directed thrust displacement also occurred along the basement–cover interface prior to out-of-synform movement. This would necessitate a reversal of movement sense along the southern contact during D_{BC} and is considered unlikely because: (1) bedding-parallel deformation zones in the lower Q_1 consistently indicate top-to-the-south movement near the southern contact and only become north-directed in the middle Q_1 (Harris in press); (2) early N-directed movement indicators are nowhere observed along this contact; and (3) intense folding of S_M, which might be expected to occur in response to movement-sense reversal, is a rare and localized feature. In addition, such folds are also present along the northern contact, where no movement-sense reversal would occur. Rare south-side-up shear zones within the Uncompahgre Group along the southern contact occur at high angles to the contact and, thus, could not have accommodated significant N-directed thrusting; they are probably conjugates to the north-side-up zones. Harris (in press) argues that the basal Q_1 remained attached to basement during thrusting and that the primary detachment(s) occurred in the upper Q_1 and overlying pelites.

The portion of the southern contact immediately east of Lime Creek (Fig. 3b) cannot be interpreted as an unconformity because the basal unit (Q_1) of the Uncompahgre Group is absent (Harris *et al.* 1987). Obliquely plunging mineral lineations and sinistral kinematic indicators (Fig. 6e) at location V suggest that this segment of the contact is a shear zone with oblique sinistral and west-side-down displacement. This interpretation is supported by the left-lateral strike separation of Q_1 (Fig. 3b) and the occurrence of sinistral kinematic indicators in the basement rocks exposed south of this area (Fig. 1b) (Harris *et al.* 1987, Gibson & Simpson 1988).

Origin of micaceous zones along basement–cover contacts

The localization of ductile deformation along the basement–cover interface implies that this zone was a mechanically weak lithologic horizon. Tewksbury (1985) suggested that these phyllitic rocks were derived from pelites of the Uncompahgre Group. Field and microscopic observations, however, indicate that many of the contact zone phyllites contain relict gneissic or plutonic textures (Figs. 5a–d & f) and were derived from the basement by alteration and deformation. Although some phyllites lack these textures and could be deformed pelites, the gradual obliteration of relict fabrics with increasing S_M intensity (Figs. 5b, c & e) and the local preservation of S_{2B} within 5 cm of the contact (Fig. 6b) suggest that this is not the case.

The presence of S_M cleavage folia transecting fine-grained aggregates of randomly oriented muscovite (Fig. 5b) shows that alteration of the basement rocks to phyllosilicate-rich lithologies occurred prior to D_{BC} deformation. Although these textures demonstrate that S_M was superimposed on previously retrograded basement rocks, syn- to post-kinematic porphyroblast textures (Fig. 6a) indicate that the present mineral assemblages are the product of syn- to post-D_{BC}, M_{BC} metamorphism. Conditions of M_{BC} have been estimated at T = 420–520°C, P = 1–3 kbar (Gibson 1987).

Rocks of the contact zones have mineral assemblages that include quartz (36–56%) and muscovite (28–50%) with common andalusite (≤14%), chloritoid (≤12%), chlorite (≤12%) and Fe/Ti-oxides (≤18%) (Table 1). Quartzo-feldspathic basement gneisses that typically occur adjacent to the contacts are composed predominantly of plagioclase (40–45%), biotite (9–16%) and quartz (32–36%) with variable proportions of potassium feldspar (≤8%), muscovite (≤6%), hornblende (≤4%) and garnet (≤1%) (Table 1). When plotted on ACF and AKF diagrams (Eskola 1915), tie lines among these phases define ranges of bulk composition for the basement and contact zone rocks in terms of the apices of each diagram (Fig. 9). Basement rock bulk compositions lie within areas bounded by the compositions of plagioclase, biotite, potassium feldspar, muscovite, hornblende, epidote and garnet (Fig. 9) that combine, in three dimensions, into an irregularly shaped compositional volume. Bulk compositions for the contact zone rocks, however, occur entirely within the AKF plane in an area bounded by the compositions of andalusite, muscovite, chlorite and chloritoid (Fig. 9). The fact that these ranges of bulk compositions do not overlap implies

Table 1. Modal mineral assemblages of basement rocks and samples from basement–cover contacts; counts of 1000 points per thin section; sample locations given in Gibson (1987)

Sample	Pl	Ksp	Qtz	Hb	Act*	Grt	Ep†	Bt	Ms	Chl‡	Ctd	And	Ox
Basement													
28	43.0	6.6	35.3	—	—	—	5.8	5.9	—	3.0	—	—	tr
29	32.9	—	tr	30.9	14.8	—	3.6	5.4	—	10.9	—	—	1.2
162	47.4§		33.1	3.0	—	tr	—	16.2	—	—	—	—	tr
180	49.0§		32.4	—	—	—	—	12.6	6.0	—	—	—	tr
327	48.1§		35.8	—	—	tr	5.3	8.6	—	1.9	—	—	tr
Contact zone													
220A	—	—	36.5	—	—	—	—	—	32.9	8.0	5.5	—	17.1
220B	—	—	2.9	—	—	—	—	—	53.5	—	41.5	—	2.1
316	—	—	55.6	—	—	—	—	—	28.8	—	—	13.7	1.9
317	—	—	45.0	—	—	—	—	—	38.6	—	4.6	6.5	5.3
326	—	—	40.1	—	—	—	—	—	44.5	11.9	—	—	3.5
412	—	—	36.9	—	—	—	—	—	50.2	—	7.5	—	5.4

*Rims around hornblende.
†Replaces plagioclase.
‡Pseudomorphs biotite in basement rock.
§Undifferentiated feldspar.

that the bulk compositions of the basement rocks along the contacts were modified during alteration.

Although a detailed study of the bulk chemical changes accompanying the transition from the basement into the contact zones has not been undertaken, several major element analyses of felsic gneisses, ~1690 Ma granites and contact zone rocks with relict basement textures are available (Barker 1969, Gibson 1987) and allow some tentative conclusions to be drawn. Graphical comparison of data from the contact zones and basement (Fig. 10) shows considerable change in the content of various oxides (e.g. Na_2O, CaO, K_2O, Al_2O_3) and implies open-system behavior during alteration. In order to facilitate discussion of oxide gains and losses, a reference frame was established by normalizing the data to 13.5 wt % Al_2O_3 (Fig. 10), which is considered to be relatively immobile in most geologic processes (Loughnan 1969, Brimhall 1979, Sinha *et al.* 1986). The normalized analyses do not total to 100%, implying that volume loss occurred during alteration. Comparison of the normalized data with those from the basement samples indicates that the contact zone rocks are depleted in SiO_2, CaO and Na_2O and enriched in volatile components (Fig. 10). Two of the three contact zone samples contain less MgO than the basement rocks, although the

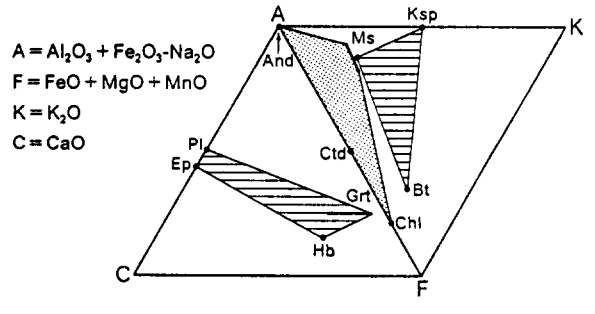

Fig. 9. ACF and AKF diagrams showing ranges of bulk composition for basement rocks (ruled) and contact zone rocks (stippled).

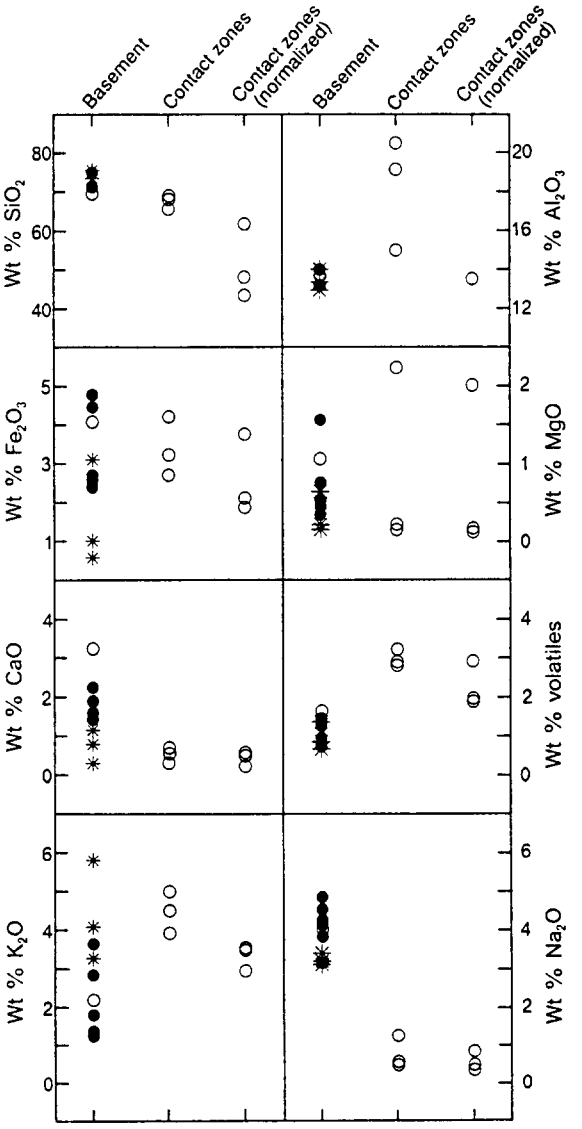

Fig. 10. Bulk-rock compositions for basement, contact zone and contact zone normalized to 13.5 wt % Al_2O_3. Analyses of gneisses (filled circle) and granites (asterisk) are from Barker (1969); other data points (open circles) are ICP analyses from Gibson (1987).

third shows enrichment. This MgO-rich analysis corresponds to sample 326 (Table 1), which contains more chlorite than is typically present in the contact zone specimens. The low MgO values are probably more typical of the contact zones because of the general scarcity of chlorite, and also imply MgO depletion. Trends in K_2O and Fe_2O_3 cannot be accurately defined because of the wide variation of these oxides in the basement rocks. However, the redistribution of Fe from silicate minerals (biotite, amphibole, garnet) in the basement rocks into magnetite within the contact zones suggests that the rocks were oxidized during the alteration process.

Alteration of the basement rocks must have involved significant fluid influx, both as a means of hydrating preexisting mineral assemblages and as a mechanism for the removal of Si^{4+}, Ca^{2+}, Mg^{2+} and Na^{+}. Such fluid interaction could have resulted from a variety of processes, including interaction with magmatic fluids (Meyer & Hemley 1967, Ferry 1985), focused fluid flow within a deformation zone (Beach 1980, Sinha *et al.* 1986) or weathering (Loughnan 1969). A magmatic origin for the fluids seems unlikely because the alteration is not spatially associated with either the 1690 or 1440 Ma intrusions, especially along the southern contact.

Retrogression within shear zones typically occurs either synchronous with or subsequent to deformation and is attributed to interaction with fluids flowing along zones of relatively high permeability (Etheridge *et al.* 1983, Rutter & Brodie 1985). Concurrent alteration of rocks outside the deforming zone may result in nearly complete preservation of relict fabrics (Beach & Tarney 1978). Well-documented examples of hydrated shear zones (Beach & Tarney 1978, Etheridge & Cooper 1981, Sandiford 1985, Sinha *et al.* 1986) display mobility of Si, Mg, Fe, Ca, Na and K. However, specific trends for individual elements vary with the physical conditions, fluid character, protolith composition and mineral breakdown reactions (cf. Beach & Tarney 1978, Beach 1980, Sinha *et al.* 1986) and are probably not themselves diagnostic of the hydrating shear-zone mechanism.

Weathering of silicate rocks involves the breakdown of feldspar, amphibole and biotite to clay minerals by either the exchange of H^{+} for bonded cations or the addition of OH^{-} to the rock-forming silicates (Loughnan 1969). The behavior of various cations during weathering depends on numerous factors, including pH, redox potential and degree of leaching by water. Under leaching conditions, Ca^{2+}, Mg^{2+}, Na^{+} and K^{+} are most readily lost from the system, although K^{+} may be 'fixed' within clay minerals and retained to higher degrees of weathering (Loughnan 1969). Si^{4+} is lost at a slower rate. In a reducing environment, Fe remains in the highly soluble ferrous state and may be thoroughly leached whereas, under oxidizing conditions, it is stabilized in the insoluble ferric state as oxide or hydroxide compounds (Loughnan 1969). Al^{3+} and Ti^{4+} are relatively immobile and are concentrated within the regolith. Deep weathering of felsic crystalline rocks typically results in a mixture composed largely of quartz, kaolinite and iron–titanium oxides and hydroxides (Loughnan 1969, Ollier 1969, Pavich 1986).

Weathering of the basement prior to deposition of the Uncompahgre Group best explains the occurrence of these micaceous zones along an inferred unconformity, the pre-deformational timing of basement alteration, and the enrichment of Al_2O_3 relative to numerous other oxides. The loss of SiO_2, MgO, CaO and Na_2O, redistribution of part of the Fe into an oxide form, and hydration of basement lithologies are consistent with the processes known to occur in a wet, oxidizing weathering zone. Preserved gneissic and granitic textures in the micaceous zones imply that the regolith was, at least in part, saprolitic. Lenses with relict original textures surrounded by a structureless, micaceous rock (Fig. 7b) are interpreted to have originated as corestones within the regolith (cf. Ollier 1969). Irregularities in the contact between the Uncompahgre Group and micaceous zone (Fig. 7) probably reflect differential erosion into the weathered horizon. The thickness of the micaceous zone is similar to those of other ancient regoliths, which range from tens of centimeters (Gay & Grandstaff 1980) to in excess of 50 m (Ross & Chiarenzelli 1985). The variable thickness of the micaceous zone may have been either inherited from original thickness variations or resulted from differential tectonic strain. Thinning during D_{BC} folding would have been least intense along gently dipping contact segments (south of Snowdon Peak, Fig. 3b), where the thickest micaceous contact zone is observed.

Modern regoliths from leaching environments are typically depleted in K^{+} and, therefore, are composed primarily of aluminous minerals, such as kaolinite or gibbsite (Loughnan 1969, Pavich 1986). In contrast, K-bearing micas, not kaolinite or aluminous metamorphic minerals such as pyrophyllite or Al_2SiO_5 polymorphs, predominate in many ancient regoliths (Matthews & Scharrer 1968, Gay & Grandstaff 1980, Button & Tyler 1981, Retallick 1986), including the contact zones in the Needle Mountains. This discrepancy between modern and ancient weathering zones has been attributed to either the incomplete leaching of K^{+} during weathering (Weaver 1969, Button & Tyler 1981) or diagenetic/metamorphic alteration of primary aluminous clay minerals to more potassic compositions (Gay & Grandstaff 1980, Palmer *et al.* 1988). If the contact zone rocks were originally more depleted in K_2O, modification of phyllosilicate compositions could have occurred by diagenetic mineral reactions (Hower *et al.* 1976) during dewatering of the Uncompahgre Group. Similarly, marked depletion of the contact zones in SiO_2 (Fig. 10) could have been due to both weathering processes and silica dissolution (Gibson 1987) during S_M formation.

CONCLUSIONS

Basement–cover contacts in the northwestern Needle Mountains are interpreted as segments of a Middle

Proterozoic unconformity with a preserved regolith. This conclusion dictates that the Uncompahgre Group is younger than the 1694 ± 20 Ma granites, which are truncated along the unconformity surface, and substantiates the stratigraphic interpretations of Barker (1969) and Harris *et al.* (1987) (Fig. 2a). It is inconsistent with the model that the basement and cover rocks were brought in contact by S-directed thrusting (Tewksbury 1985) (Fig. 2b).

The results of this study emphasize the need for detailed examination of contacts between contrasting lithologic suites in deformed terranes. Deformed regoliths may be preserved as zones of muscovite-rich rock along major lithologic boundaries (see also Barrientos & Selverstone 1987). The inherent mechanical weakness of these micaceous rocks can localize deformation and lead to the development of complex structures along basement–cover contacts, even though the contacts are fundamentally stratigraphic in origin. The presence of deformation zones along basement–cover contacts, therefore, does not necessarily imply that the adjacent lithologies were tectonically juxtaposed. Petrographic and kinematic analysis of these zones may help to distinguish them from major fault boundaries and lead to a clearer understanding of their significance with respect to the stratigraphic and tectonic evolution of a region.

Acknowledgements—This work was funded by National Science Foundation grant EAR-8507052 to C. Simpson and teaching assistantships and a Cunningham Research Fellowship from Virginia Polytechnic Institute and State University (1986–1987) to the author. Discussions with C. W. Harris were valuable throughout the study. C. Simpson, K. A. Eriksson, L. Glover III and one anonymous reviewer provided helpful comments on the manuscript.

REFERENCES

American Geological Institute. 1980. *Glossary of Geology* (2nd edn) (edited by Bates, R. L. & Jackson, J. A.). Am. Geol. Inst., Falls Church, Virginia.

Baars, D. L. & See, P. D. 1968. Pre-Pennsylvanian stratigraphy and paleotectonics of the San Juan Mountains, southwestern Colorado. *Bull. geol. Soc. Am.* **79**, 333–350.

Barker, F. 1969. Precambrian geology of the Needle Mountains, southwestern Colorado. *Prof. Pap. U. S. geol. Surv.* **644-A**, 1–33.

Barker, F., Peterman, Z. E. & Hildreth, R. A. 1969. A rubidium–strontium study of the Twilight Gneiss, W. Needle Mountains, Colorado. *Contr. Miner. Petrol.* **23**, 271–282.

Barrientos, X. & Selverstone, J. 1987. Metamorphosed soils as stratigraphic indicators in deformed terranes: an example from the eastern Alps. *Geology* **15**, 841–844.

Beach, A. 1980. Retrogressive metamorphic processes in shear zones with special reference to the Lewisian complex. *J. Struct. Geol.* **2**, 257–263.

Beach, A. & Tarney, J. 1978. Major and trace element patterns established during retrogressive metamorphism of granulite facies gneisses, NW Scotland. *Precambrian Res.* **7**, 325–348.

Bickford, M. E., Wetherill, G. W., Barker, F. & Chin-Nan Lee-Hu. 1969. Precambrian Rb–Sr chronology in the Needle Mountains, southwestern Colorado. *J. geophys. Res.* **74**, 1660–1676.

Brimhall, G. H. Jr. 1979. Lithologic determination of mass transfer mechanisms of multiple-stage porphyry copper mineralization at Butte, Montana: vein formation by hypogene leaching and enrichment of potassium–silicate protore. *Econ. Geol.* **74**, 556–589.

Button, A. & Tyler, N. 1981. The character and economic significance of Precambrian paleoweathering and erosion surfaces in southern Africa. *Econ. Geol. (75th Anniversary Volume)* **75**, 686–709.

Coney, P. J. 1980. Cordilleran metamorphic core complexes: an overview. In: *Cordilleran Metamorphic Core Complexes* (edited by Crittenden, M. D., Coney, P. J. & Davis, G. H.). *Mem. geol. Soc. Am.* **153**, 7–31.

Cross, W., Howe, E., Irving, J. D. & Emmons, W. 1905. Description of the Needle Mountains Quadrangle, Colorado. *U. S. Geol. Surv. Atlas*, Folio 131.

Dahlstrom, C. D. A. 1977. Structural geology in the eastern margin of the Canadian Rocky Mountains. *29th Annual Field Conf., Wyoming Geol. Assn Guidebook*, 407–439.

Eskola, P. 1915. On the relations between the chemical and mineralogical composition in the metamorphic rocks of the Orijarvi region. *Bull. Comm. geol. Finlande* **44**.

Etheridge, M. A. & Cooper, J. A. 1981. Rb–Sr isotopic and geochemical evolution of a recrystallized shear (mylonite) zone at Broken Hill. *Contr. Miner. Petrol.* **78**, 74–84.

Etheridge, M. A., Wall, V. J. & Vernon, R. H. 1983. The role of the fluid phase during regional metamorphism and deformation. *J. metamorph. Geol.* **1**, 205–226.

Ferry, J. M. 1985. Hydrothermal alteration of Tertiary igneous rocks from the Isle of Skye, NW Scotland II. granites. *Contr. Miner. Petrol.* **91**, 283–304.

Gay, A. L. & Grandstaff, D. E. 1980. Chemistry and mineralogy of Precambrian paleosols at Elliot Lake, Ontario, Canada. *Precambrian Res.* **12**, 349–373.

Gee, D. G. 1980. Basement-cover relationships in the central Scandinavian Caledonides. *Geol. För. Stockh. Förh.* **102**, 455–474.

Gibson, R. G. 1987. Structural studies in a Proterozoic gneiss complex and its adjacent cover rocks, West Needle Mountains, Colorado. Unpublished Ph.D. dissertation, Virginia Polytechnic Institute and State University, Blacksburg, Virginia.

Gibson, R. G. & Harris, C. W. In press. Geologic map of Proterozoic rocks in the northwestern Needle Mountains, Colorado. *Geol. Soc. Am. Map and Chart Series.*

Gibson, R. G. & Simpson, C. 1988. Proterozoic polydeformation in basement rocks of the Needle Mountains, Colorado. *Bull. geol. Soc. Am.* **100**, 1957–1970.

Gratier, J.-P. & Vialon, P. 1980. Deformation patterns in a heterogeneous material: folded and cleaved sedimentary cover immediately overlying a crystalline basement (Oisans, French Alps). *Tectonophysics* **65**, 151–180.

Harris, C. W. 1987. A sedimentological and structural analysis of the Proterozoic Uncompahgre Group, Needle Mountains, Colorado. Unpublished Ph.D. dissertation, Virginia Polytechnic Institute and State University, Blacksburg, Virginia.

Harris, C. W. In press. Polyphase suprastructure deformation in metasedimentary rocks of the Uncompahgre Group: remnant of a Proterozoic fold belt in southwest Colorado. *Bull. geol. Soc. Am.*

Harris, C. W. & Eriksson, K. A. 1987. Tide-, storm-, and wave-influenced shelf sedimentation in a tectonically active intracratonic basin: the Proterozoic Uncompahgre Group, SW Colorado. *Geol. Soc. Am. Abs. w. Prog.* **19**, 281–282.

Harris, C. W., Gibson, R. G., Simpson, C. & Eriksson, K. A. 1987. Proterozoic cuspate basement-cover structure, Needle Mountains, Colorado. *Geology* **15**, 950–953.

Hower, J., Eslinger, E. V., Hower, M. E. & Perry, E. A. 1976. Mechanism of burial metamorphism of argillaceous sediment: 1. mineralogical and chemical evidence. *Bull. geol. Soc. Am.* **87**, 725–737.

Jacob, R. E., Snowdon, P. A. & Bunting, F. J. L. 1983. Geology and structural development of the Tumas basement dome and its cover rocks. *Spec. Publ. geol. Soc. S. Afr.* **11**, 157–172.

Lambert, M. B. & van Staal, C. R. 1987. Archean granite-greenstone boundary relationships in the Beaulieu River volcanic belt, Slave Province, N. W. T. In: *Current Research, Part A. Geol. Surv. Can. Pap.* **87-1A**, 605–618.

Loughnan, F. C. 1969. *Chemical Weathering of the Silicate Minerals.* American Elsevier Publishing Co., New York.

Matthews, P. E. & Scharrer, R. H. 1968. A graded unconformity at the base of the Early Precambrian Pongola system. *Trans. geol. Assn S. Afr.* **71**, 257–273.

Meyer, C. & Hemley, J. J. 1967. Wall Rock Alteration. In: *Geochemistry of Hydrothermal Ore Deposits* (edited by Barnes, H. L.). Holt, Rinehard and Winston, Inc., New York, 166–235.

Ollier, C. 1984. *Weathering* (2nd edn). Longman, London.

Passchier, C. W. & Simpson, C. 1986. Porphyroclast systems as kinematic indicators. *J. Struct. Geol.* **8**, 831–843.

Pavich, M. J. 1986. Processes and rates of saprolite production and erosion on a foliated granitic rock of the Virginia Piedmont. In: *Rates of Chemical Weathering of Rocks and Minerals* (edited by

Colman, S. M. & Dethier, D. P.). Academic Press, Orlando, 552–590.

Palmer, J. A., Phillips, G. N. & McCarthy, T. S. 1988. Paleosols and their relevance to Precambrian atmospheric composition. *J. Geol.* **97**, 77–92.

Platt, J. P. 1983. Progressive refolding in ductile shear zones. *J. Struct. Geol.* **5**, 619–622.

Powell, C. McA. 1979. A morphological classification of rock cleavage. *Tectonophysics* **58**, 21–34.

Ramsay, J. G. 1962. The geometry and mechanics of formation of "similar" type folds. *J. Geol.* **70**, 309–327.

Ramsay, J. G. 1967. *Folding and Fracturing of Rocks.* McGraw-Hill, New York.

Retallick, G. J. 1986. The fossil record of soils. In: *Paleosols, Their Recognition and Significance* (edited by Wright, V. P.). Princeton University Press, Princeton, 1–57.

Ross, G. M. & Chiarenzelli, J. R. 1985. Paleoclimatic significance of widespread Proterozoic silcretes in the Bear and Churchill Provinces of the northwestern Canadian Shield. *J. sedim. Petrol.* **55**, 196–204.

Rutter, E. H. & Brodie, K. H. 1985. The permeation of water into hydrating shear zones. In: *Metamorphic Reactions, Kinetics, Textures and Deformation* (edited by Thompson, A. B. & Rubie, D. C.). Springer-Verlag, New York, 242–250.

Sandiford, M. 1985. The origin of retrograde shear zones in the Napier Complex: implications for the tectonic evolution of Enderby Land, Antarctica. *J. Struct. Geol.* **7**, 477–488.

Schmid, S. M. & Casey, M. 1986. Complete texture analysis of commonly observed quartz c-axis patterns. In: *Mineral and Rock Deformation: Laboratory Studies* (edited by Hobbs, B. E. & Heard, H. C.). *Am. Geophys. Un. Geophys. Monogr.* **36**, 263–286.

Silver, L. T. & Barker, F. 1968. Geochronology of Precambrian rocks of the Needle Mountains, southwestern Colorado, part I, U–Pb zircon results. *Spec. Pap. geol. Soc. Am.* **115**, 204–205.

Simpson, C. & Schmid, S. M. 1983. An evaluation of criteria to deduce the sense of movement in sheared rocks. *Bull. geol. Soc. Am.* **94**, 1281–1288.

Sinha, A. K., Hewitt, D. A. & Rimstidt, J. D. 1986. Fluid interaction and element mobility in the development of ultramylonites. *Geology* **14**, 883–886.

Spoelhof, R. W. 1976. Pennsylvanian stratigraphy and paleotectonics of the western San Juan Mountains, southwestern Colorado. In: *Studies in Colorado Field Geology* (edited by Epis, R. C. & Weimer, R. J.). *Colorado School of Mines Prof. Contr.* **8**, 159–179.

Tewksbury, B. J. 1985. Revised interpretation of the age of allochthonous rocks of the Uncompahgre Formation, Needle Mountains, Colorado. *Bull. geol. Soc. Am.* **96**, 224–232.

Weaver, C. E. 1969. Potassium, illite and the ocean. *Geochim cosmochim. Acta.* **31**, 2181–2196.